Nonstandard quantum interference graphene rings and disks

Adam Rycerz
Marian Smoluchowski Institute of Physics, Jagiellonian University, Kraków, Poland

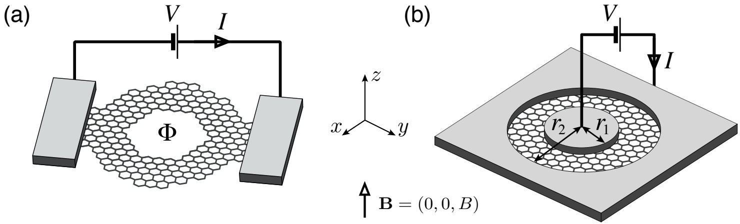

Montréal, Canada, October 14-16, 2015

Emergent Dirac fermions in graphene

4 August 1972, Volume 177, Number 4047

SCIENCE

More Is Different

Broken symmetry and the nature of the hierarchical structure of science.

P. W. Anderson

The reductionist hypothesis may still be a topic for controversy among philosophers, but among the great majority of active scientists I think it is accepted planation of phenomena in terms of known fundamental laws. As always, distinctions of this kind are not unambiguous, but they are clear in most cases. Solid state physics, plasma physics, and perhaps

What differs graphene from a collection of carbon atoms?

- The **valley pseusospin** ($\Rightarrow$ *fermion doubling*)
- Time-reversal symmetry breaking at zero magnetic field
- Pseudodiffusive charge transport and more ...

Emergent Dirac fermions and valleys

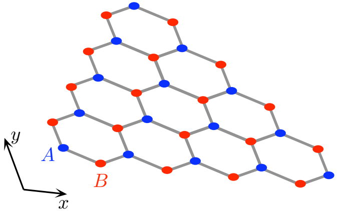

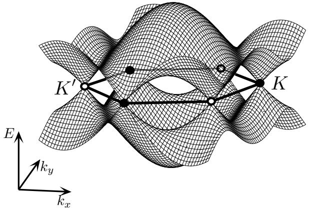

Tight-binding Hamiltonian:

$$\mathcal{H}_{\rm TBA} = \sum_{\langle ij \rangle} \left[\, t_{ij}(\mathbf{A}) |i\rangle\langle j| + \text{h.c.} \,\right],$$

$$t_{ij}(\mathbf{A}) = -t \exp\left[i \frac{2\pi}{\Phi_0} \int_{\mathbf{r}_i}^{\mathbf{r}_j} \mathbf{A} \cdot d\mathbf{r} \right],$$

$t \approx 3\,$eV, and $\Phi_0 = h/e$.

Envelope wavefunction:

$$\Psi(\mathbf{r}) = \begin{pmatrix} \psi_A \\ \psi_B \end{pmatrix} e^{i\mathbf{K}\cdot\mathbf{r}} + \begin{pmatrix} \psi'_A \\ \psi'_B \end{pmatrix} e^{i\mathbf{K}'\cdot\mathbf{r}}.$$

For K-point and $\mathbf{A} = 0$:

$$\frac{\hbar v_F}{i} \begin{pmatrix} 0 & \partial_x - i\partial_y \\ \partial_x + i\partial_y & 0 \end{pmatrix} \begin{pmatrix} \psi_A \\ \psi_B \end{pmatrix} = E \begin{pmatrix} \psi_A \\ \psi_B \end{pmatrix},$$

with $v_F \equiv \frac{\sqrt{3}}{2} ta/\hbar \approx 10^6$ m/s, $a = 0.246\,$nm.

A compact form: $H_0\Psi = E\Psi$, with $H_0 = v_F \boldsymbol{\sigma} \cdot \boldsymbol{p}$, $\boldsymbol{\sigma} = (\sigma_x, \sigma_y)$, and $\boldsymbol{p} = -i\hbar(\partial_x, \partial_y)$. For $B \neq 0$: $\boldsymbol{p} \rightarrow \boldsymbol{p} - \frac{e}{c}\boldsymbol{A}$.

Valleytronics in graphene

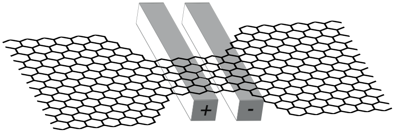

AR, Tworzydło, Beenakker, Nat. Phys. (2007)

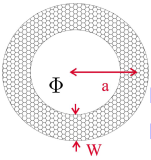

Recher *et al.*, PRB **76**, 235404 (2007)

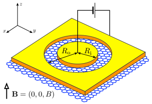

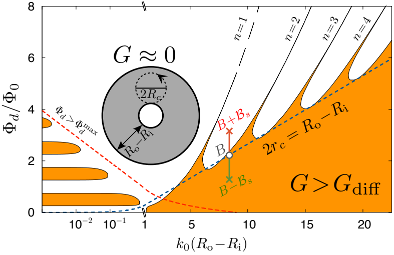

AR, PRB **81**, 121404(R) (2010);
Khatibi *et al.*, PRB **88**, 195426 (2013).
Related: Fujita et al., APL **97**, 043508 (2010)

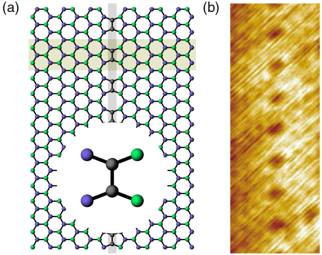

Gunlycke and White, PRL **106**, 136806 (2011)

Breaking the valley degeneracy

- Lowest mode in constriction w/zigzag edges, domain walls in BLG, etc. [$\Rightarrow$ *not this talk ...*]
- Aharonov-Bohm rings [$\Rightarrow$ Recher, Trauzettel, AR *et al.*, PRB **76**, 235404 (2007)]

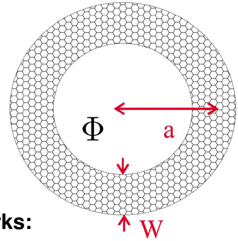

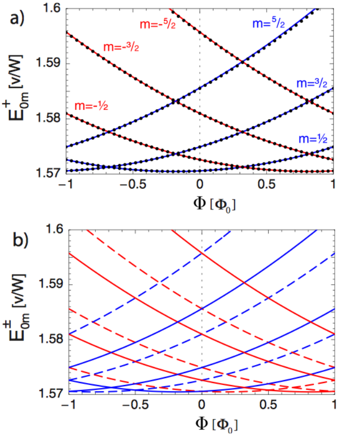

Related works:

Xu *et al.*, Sci. Rep. **5**, 8963 (2015); Culcer *et al.*, PRL **108** 126804 (2012); Pályi and Burkard, PRL **106** 086801 (2011); Recher *et al.*, PRB **79**, 085407 (2009); . . .

The condensed-matter two-slit experiment

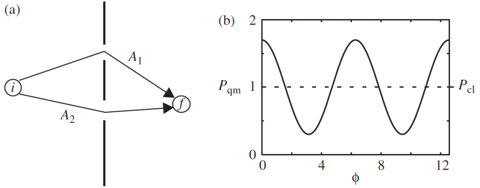

Two-slit experiment. Quantum interference between two trajectories (a) results in oscillatory dependence of the propagation probability on the phase shift between two amplitudes ((b), plotted for $P_1/P_2 = 6$).

⇒ In metallic (or semiconducting) Aharonov-Bohm rings one cannot neglect *looped* trajectories. This may effect the oscillation period [Sharvin and Sharvin, JETP Lett. **34**, 272 (1981); Webb et al., PRL **54**, 2696 (1985).]

⇒ Fourier analysis necessary to determine the character of interference in a given A-B ring.

[Image from: Nazarov and Blanter, *Quantum Transport: Introduction to Nanoscience,* Cambridge University Press (Cambridge, 2009).]

Aharonov-Bohm effect in graphene rings

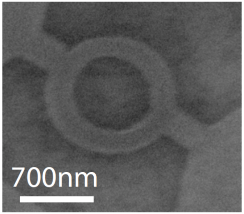

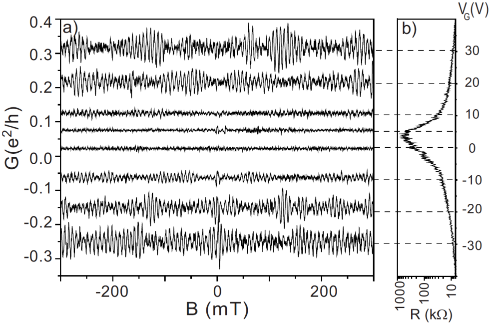

⇒ In graphene A-B rings, experiments show oscillations with the standard $\Phi_0 = h/e$ period, and the magnitude $\Delta G \propto G$ (and also $\Delta G \propto T^{-1/2}$), indicating the *tunneling* transport regime [Russo et al., PRB **77**, 085413 (2008); Stampfer et al., Int. J. Mod. Phys. **23**, 2647 (2009).]

A-B effect and valley polarization

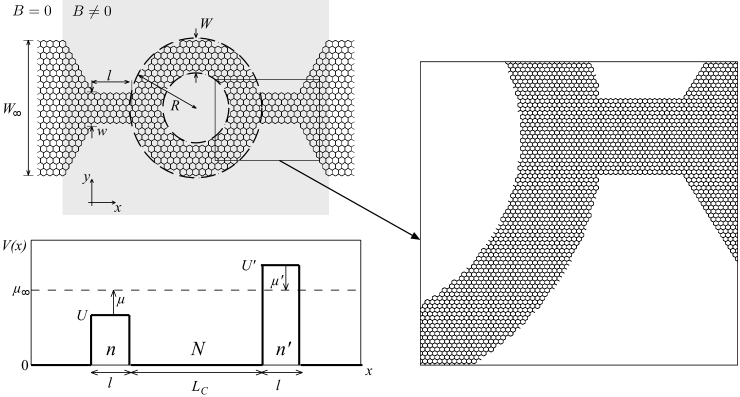

AR, Acta Phys. Polon. A **115**, 322 (2009).

Related works: Zarenia *et al.*, PRB **81**, 045431 (2010); Wurm *et al.*, Semicond. Sci. Technol. **25**, 034003 (2010); Schelter *et al.*, PRB **81**, 195441 (2010).

A-B effect and valley polarization

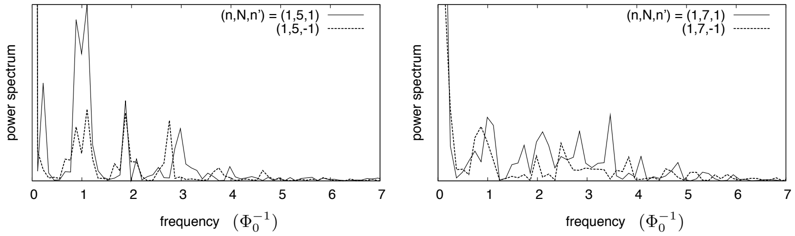

[AR, Acta Phys. Polon. A **115**, 322 (2009)]

$\Rightarrow$ Tunneling regime ($\Delta G \propto G$) reproduced in simulations when disorder taken into account [Wurm et al. (2010)].

$\Rightarrow$ *Frequency doubling* upon inversion of valley polarity (in one constriction only) not yet observed.

The Corbino disk in graphene

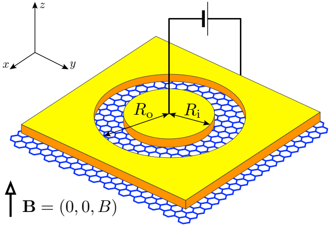

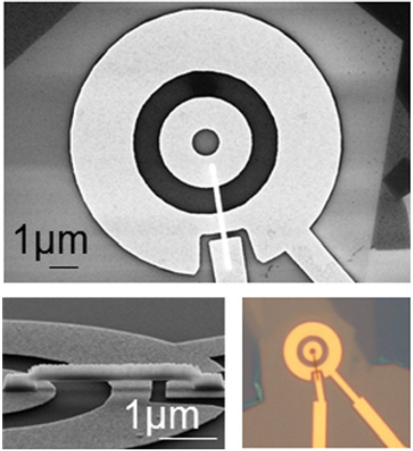

Bottom left: AR, PRB **81**, 121404(R) (2010). *Right:* Peters et al., APL **104**, 203109 (2014).

Magnetoconductance of the Corbino disk in MLG

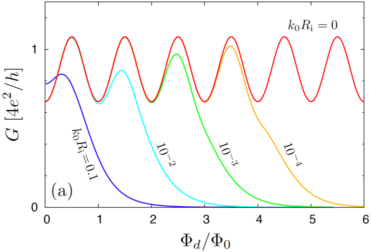

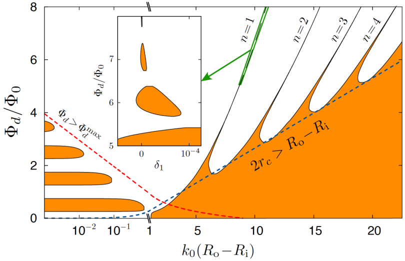

- Periodic, approximately sinusoidal, conductance oscillations [with the period $\Phi_0 = 2(h/e)\mathcal{L}$, $\mathcal{L} = \ln(R_o/R_i)$] appear if $|\Phi_d| \lesssim \Phi_d^{\max} = -(2h/e)\ln(k_0 R_i)$, where $\Phi_d = \pi B(R_o^2 - R_i^2)$ and $k_0 = |E_F|/(\hbar v_F)$. / $\Rightarrow$Similarly – for higher LLs. /
- Conductance for the Dirac point ($k_0 \rightarrow 0$) reads $G = G_{\rm diff} + \sum_{m=1}^{\infty} G_m \cos(2\pi m\Phi_d/\Phi_0)$, where $G_{\rm diff} = 2g_0/\mathcal{L}$, $G_m = 4\pi^2(-)^m m g_0/(\mathcal{L}^2 \sinh(\pi^2 m/\mathcal{L}))$, and $g_0 = 4e^2/h$.

[AR, PRB **81**, 121404(R) (2010); fig-s are for $R_o/R_i = 10$.]

Trigonal warping in bilayer graphene

- Landauer conductivity [Snyman & Beenakker, 2007], $\gamma_3 = \gamma_4 = 0$:

$$\sigma_{\rm bilayer} = GL/W = 2\sigma_0$$

- Kubo conductivity [Cserti et al., 2007], $\gamma_3 \neq 0$:

$$\sigma_{\rm bilayer} = 6\sigma_0 \text{ (!)}$$

- *Experiment:* [Mayorov et al., 2011] $\sigma_{\rm bilayer} \simeq 5\sigma_0$.

[*$\sigma_0 = (4/\pi)e^2/h$ – universal conductivity of a monolayer.*]

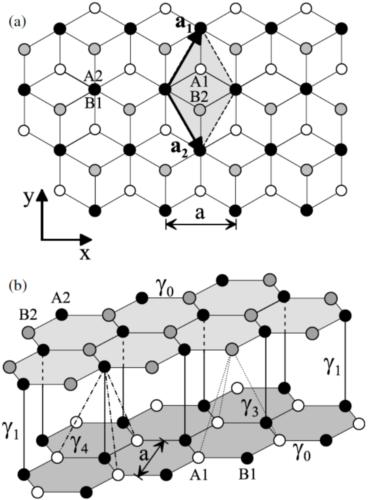

Rep. Prog. Phys. **76** (2013) 056503 E McCann and M Koshino

Table 1. Values (in eV) of the SWM model parameters [64–67] determined experimentally. Numbers in parentheses indicate estimated accuracy of the final digit(s). The energy difference between dimer and non-dimer sites in the bilayer is $\Delta' = \Delta - \gamma_2 + \gamma_5$. Note that next-nearest layer parameters γ_2 and γ_5 are not present in bilayer graphene.

Parameter	Graphite [67]	Bilayer [76]	Bilayer [55]	Bilayer [56]	Bilayer [80]	Trilayer [82]
γ_0	3.16(5)	2.9	3.0[a]	—	3.16(3)	3.1[a]
γ_1	0.39(1)	0.30	0.40(1)	0.404(10)	0.381(3)	0.39[a]
γ_2	−0.020(2)	—	—	—	—	−0.028(4)
γ_3	0.315(15)	0.10	0.3[a]	—	0.38(6)	0.315[a]
γ_4	0.044(24)	0.12	0.15(4)	—	0.14(3)	0.041(10)
γ_5	0.038(5)	—	—	—	—	0.05(2)
Δ	−0.008(2)	—	0.018(3)	0.018(2)	0.022(3)	−0.03(2)
Δ'	0.050(6)	—	0.018(3)	0.018(2)	0.022(3)	0.046(10)

[a] This parameter was not determined by the given experiment, the value quoted was taken from previous literature.

[55] Zhang *et al.*, Phys. Rev. B **78**, 235408 (2008).
[56] Li *et al.*, Phys. Rev. Lett. **102**, 037403 (2009).
[67] Dresselhaus & Dresselhaus, Adv. Phys. **51**, 1 (2002).
[76] Malard *et al.*, Phys. Rev. B **76**, 201401(R) (2007).
[80] Kuzmenko *et al.*, Phys. Rev. B **80**, 165406 (2009).
[82] Taychatanapat *et al.*, Nature Phys. **7**, 621 (2011).

⇒ Novel phenomena governed solely by γ_3 VERY desired!

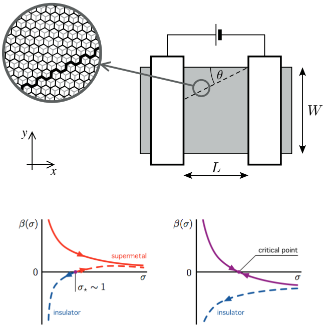

Fig. 1: (Colour on-line) Schematic scaling functions $\beta(\sigma)$ (3) for two-dimensional disordered Dirac (solid lines) and spin-orbit (dashed lined) systems. Left: noninteracting case [17]; right: Coulomb interaction included [19]. Arrows indicate the flows of the dimensionless conductivity σ with increasing L.

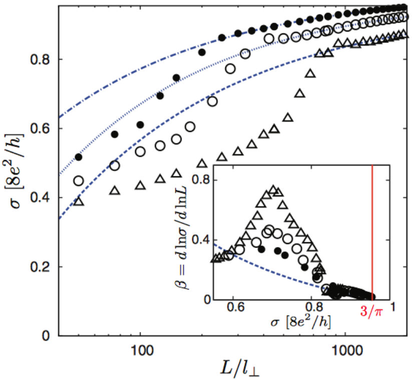

Fig. 3: (Colour on-line) Minimal conductivity of an unbiased graphene bilayer as a function of the sample length L (specified in units of $l_\perp = \hbar v_F/t_\perp \simeq 1.60\,\mathrm{nm}$). Different datapoints correspond to different values of the next-nearest neighbor interlayer hopping: $t' = 0.1\,\mathrm{eV}$ (△), $0.2\,\mathrm{eV}$ (○), and $0.3\,\mathrm{eV}$ (●).

Grzegorz Rut & AR:
⇒ PRB **89**, 045421 (2014)
⇒ EPL **107**, 47005 (2014)

[Notation: $t' \equiv \gamma_3$]

Magnetoconductance of BLG disk: t'=0

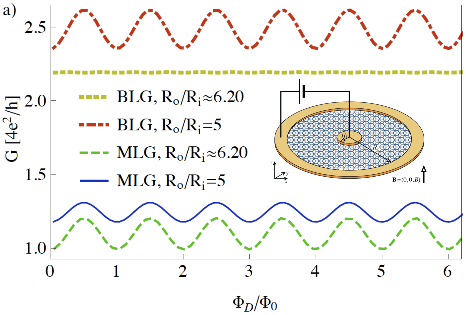

$$\Phi_D = \pi B (R_{\rm o}^2 - R_{\rm i}^2),$$

$$\Phi_0 = 2(h/e)\ln(R_{\rm o}/R_{\rm i}),$$

$$G_{\rm diff}^{BLG} = 2G_{\rm diff}^{MLG} = \frac{8e^2}{h}\frac{1}{\ln(R_{\rm o}/R_{\rm i})}.$$

⇒ Oscillations magnitude at the Dirac point: $0 \leqslant \Delta G^{\rm BLG} \leqslant 2\Delta G^{\rm MLG}$.

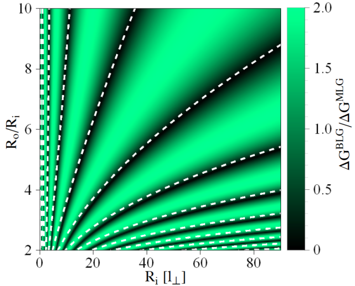

⇒ The oscillations vanish ($\Delta G^{\rm BLG} = 0$) for $R_{\rm o}/R_{\rm i} \simeq [R_{\rm i} t_\perp/(2\hbar v_F)]^{4/p}$, with $p = 1, 3, 5, \ldots$.

Magnetotransport in BLG disk: t'≠0

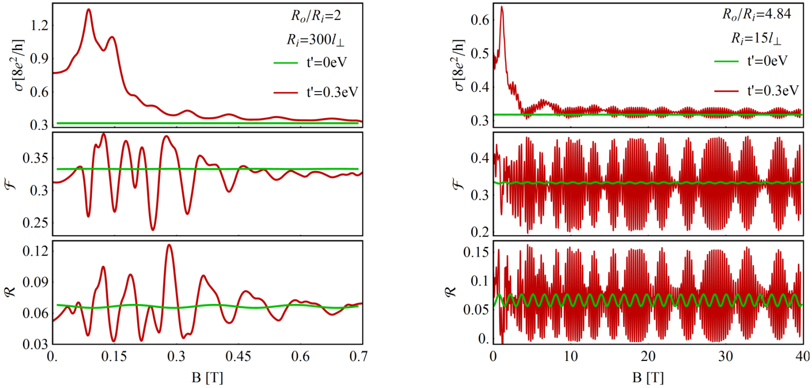

⇒ The *excess conductance decays* as $G_{\rm diff}(t') - G_{\rm diff}(0) \propto 1/B$ above the crossover field $B_\star \approx 2\hbar t'/(eL)$.

⇒ However, the *beats* remain, with $T_{\rm beat} \propto \sqrt{B}$.

[Grzegorz Rut & AR, unpublished.]

Conclusions & Acknowledgments

- Both the conductivity scaling with a sample size and the single-device magnetoconductance spectrum of BLG Corbino disk may allow one to determine skew-interlayer hopping γ_3.
- A 'common wisdom' saying that *the trigonal warping has no effect starting from few-Tesla fields* is put in question.

Collaboration:

Grzegorz Rut (PhD student)

Funding:

FNP
Foundation for Polish Science

PL GRID

NATIONAL SCIENCE CENTRE
POLAND

Project web site: http://th.if.uj.edu.pl/∼adamr/sonata.html